

Measuring Retinal Vessel Tortuosity in 10-Year-Old Children: Validation of the Computer-Assisted Image Analysis of the Retina (CAIAR) Program

Christopher G. Owen,¹ Alicja R. Rudnicka,¹ Robert Mullen,² Sarah A. Barman,² Dorothy Monekosso,² Peter H. Whincup,¹ Jeffrey Ng,³ and Carl Paterson⁴

PURPOSE. To examine the agreement of a novel computer program measuring retinal vessel tortuosity with subjective assessment of tortuosity in school-aged children.

METHODS. Cross-sectional study of 387 retinal vessels (193 arterioles, 194 veins) from 28 eyes of 14 children (aged 10 years). Retinal digital images were analyzed using the Computer Assisted Image Analysis of the Retina (CAIAR) program, including 14 measures of tortuosity. Vessels were graded (from 0 = none; to 5 = tortuous) independently by two observers. Interobserver agreement was assessed by using κ statistics. Agreement with all 14 objective measures was assessed with correlation/regression analyses. Intersession repeatability (comparing morning and afternoon sessions) of tortuosity indices was calculated.

RESULTS. Interobserver agreement of vessel tortuosity within one grade was high ($\kappa = 0.97$), with total agreement in 56% of grades and 42% differing by ± 1 grade. Tortuosity indices based on subdivided chord length methods showed strong log-linear associations with agreed subjective grades (typically $r > 0.6$; $P < 0.001$). An approach that averages the distance from the vessel to chord length along the length of the vessel showed best agreement ($r = 0.8$; $P < 0.0001$). Tortuosity measures based on curvature performed less well. Intersession repeatability of the vessel to chord technique was good, differing by values equivalent to < 1 in subjective grade.

CONCLUSIONS. Tortuosity indices based on changes in subdivided chord lengths showed optimal agreement with subjective assessment. The relation of these indices to ethnicity and cardiovascular risk factors in childhood should be examined further, as these indices may be a useful indicator of early vascular function. (*Invest Ophthalmol Vis Sci.* 2009;50:2004–2010) DOI:10.1167/iovs.08-3018

From the ¹Division of Community Health Sciences, St. George's, University of London, London, United Kingdom; the ²School of Computing Information Systems and Mathematics, Kingston University, Kingston-upon-Thames, United Kingdom; the Departments of ³Bio-engineering and ⁴Physics, Imperial College London, South Kensington Campus, London, United Kingdom.

Supported by a grant from the BUPA Foundation. The Child Heart and Health Study in England (CHASE) was supported by Grant 068362/Z/02/Z from the Wellcome Trust.

Submitted for publication October 16, 2008; revised December 15, 2008; accepted March 16, 2009.

Disclosure: C.G. Owen, None; A.R. Rudnicka, None; R. Mullen, None; S.A. Barman, None; D. Monekosso, None; P.H. Whincup, None; J. Ng, None; C. Paterson, None

The publication costs of this article were defrayed in part by page charge payment. This article must therefore be marked "advertisement" in accordance with 18 U.S.C. §1734 solely to indicate this fact.

Corresponding author: Christopher G. Owen, Cranmer Terrace, London SW17 0RE, UK; cowen@sgul.ac.uk.

The morphologic characteristics of vessels of the retina have been associated with cardiovascular and coronary disease in adult life,^{1–5} and with retinopathy of prematurity in infancy.⁶ The caliber of retinal microvasculature has also been associated with cardiovascular risk factors in childhood.^{7,8} However, the different methods of determining vessel edges and summarizing vessel width may hinder absolute comparisons of vessel dimensions between studies.^{9–12} It has been proposed that the measurement of vessel tortuosity may offer a more robust form of assessment, relying only on the identification of vessel axes as opposed to the exact location of vessel edges.¹³ Previous methods of formally describing vessel tortuosity have relied on vessel-to-chord length ratios and local curvature estimates.^{13,14} These measurements require a high level of operator involvement and are labor intensive, precluding their use in large population studies. With advances in computational technology alternative indices for quantifying absolute levels of vessel tortuosity have been developed.^{6,15–18}

Although retinal vessel tortuosity has been associated with retinopathy of prematurity and size at birth,^{18,19} whether early changes in retinal vessel tortuosity are related to cardiovascular risk factors in early life and are predictors of vascular disease in later life remains unclear. A recent study has suggested that ethnic differences in retinal vessel morphology may be an early sign of differences in endothelial function that are associated with risk factors for diabetes in childhood.²⁰ We set out to evaluate the application of the Computer Assisted Image Analysis of the Retina (CAIAR) program, previously validated in infants with retinopathy of prematurity,¹⁸ to examine the tortuosity of retinal vessels in 9- to 10-year-old children. The program returns 14 measures of vessel tortuosity, and earlier work in infants has shown a modest correlation ($r = 0.4$) between these measures and subjective assessment. We compared these indices with subjective assessment in children, to find the index that agrees optimally in this age group.

METHODS

Study Population

This investigation was performed during the Child Heart Health Study in England (CHASE), a cardiovascular health survey in 200 primary schools in London, Birmingham, and Leicester.²¹ The present report is based on 14 children recruited from one primary school in North-East London and studied during September 2007. The study of repeated measures was performed in 19 pupils from 10 primary schools who were measured both in the morning and afternoon on the same day between September 2007 and March 2008 by the same observer; afternoon assessments were made without reference to the morning measurements. Parental questionnaires were distributed (acquiring ethnic information) and clinical assessment (including physical measurements and blood sampling) performed. Ocular assessments included the measurement of vision, visual acuity, open-field autorefractometry (without cycloplegia), noncontact ocular biometry, and fundus imaging. Only details of fundus imaging are presented. The study was

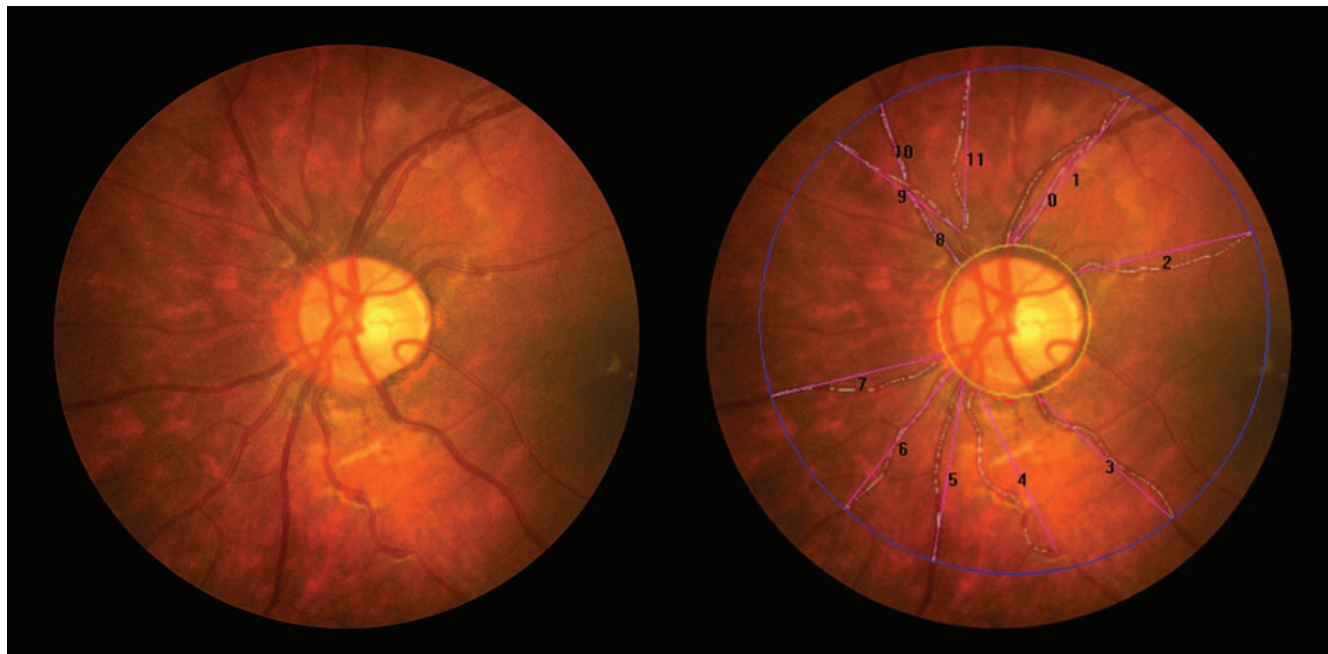


FIGURE 1. A raw 1280×1024 -pixel image (*left*), overlaid with output from the algorithm (*right*) showing vessel segments (labeled 0-11), axis points along the vessel (*white*), and chord lengths (*purple*), in a South Asian child. Vessels were measured from the *yellow circle* (fixed at 120 pixels in diameter) centered on the optic disc.

performed in accordance with the tenets of the Declaration of Helsinki and with the approval from relevant research ethics committees and informed written consent from all participants.

Imaging the Retina

A minimum of two digital images (30° , 1280×960 pixels) of the retina of each child's eye were recorded (by one of three members of the field team) with the handheld fundus camera (NM-200-D; Nidek Co., Ltd., Gamagori, Japan). Images were captured in subdued lighting, by using flash and illumination settings of $3'$; levels were adjusted by the operator in the event of perceived over- or underexposure. The camera's refractive setting was adjusted to the best vision sphere calculated from the open-field autorefractometer, only if the child's refraction was more than 4 D of hypermetropia or myopia (in reality the refractive setting was unchanged, as there was no appreciable refractive error in this sample). A fixation target was used, and focused images were captured centered on the optic disc with full field illumination. Images were displayed immediately on a color screen, allowing image capture to be repeated by the operator in the event of poor quality and were saved in tagged image file (TIF) format.

Subjective Assessment

Images were viewed "on screen" at a magnification of 10 pixels/cm (working distance, 50 cm). Vessel segments of interest identified by the software were located in the raw image (Fig. 1) and graded for tortuosity by two observers (CGO, ARR) independently, using a specially derived grading scale. This scale (based on integer values from 0 to 5) was based on sinusoidal wave forms of decreasing wavelength but identical amplitude (compared to grade 1, wavelengths decreased by a half, third, fourth, and fifth for grades 2 to 5, respectively), perceived as being indicative of the vessels being assessed (Fig. 2). Disagreements between observers >1 grade, were reassessed until agreement within ± 1 grade was reached. The mean of the 2 grades (which included noninteger values when grades differed by only 1) were compared to objective measures of tortuosity. Observers also classified vessels of interest as arterioles or venules and the degree of vessel branching (i.e., whether the vessel segment was a primary, secondary, or tertiary branch from the beginning of the measurement area).

Image Processing

Image processing was performed by using the CAIAR program. Details of the program have been reported elsewhere.¹⁸ In brief, the program identifies vessel segments (typically between 10 and 16 per eye, with the option of manual editing if any vessel is inappropriately identified) and returns 14 measures of tortuosity for each segment (12 based on changes in subdivided chord lengths, 2 on angular change in curvature).^{18,22} An example of the operation of the program is given in Figure 1. The program also analyses the mean width of vessel segments, estimated from the maximum-likelihood model fitting; data on vessel width are not presented in detail in this report. The tortuosity measures are derived from vessel axes identified by the program using maximum-likelihood fitting and connected into a continuous line. Earlier methods of quantifying vessel tortuosity have used vessel-to-chord length ratios.²² In the CAIAR program, the halfway point along the chord of a given vessel segment identified is found, resulting in two vessel segments. This process is repeated until the chord length is less than 4 pixels. The change in chord length between successive divisions of the vessel is used to obtain two sets of measurements based on level-wise indices that quantify the total increase in chord length between successive levels and segment-wise measures that determine the increase in chord length after each bisection. The tortuosity mea-

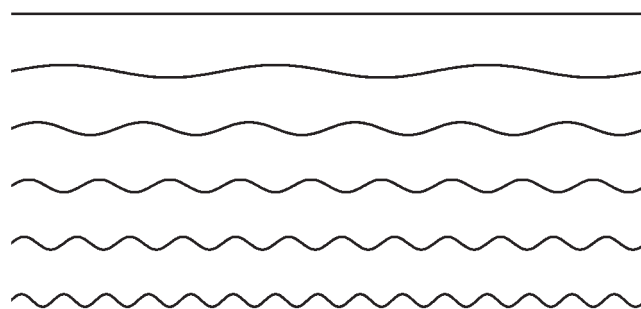


FIGURE 2. Schematic diagram used to assist in subjectively grading vessel segments from 0 (none; *top*) to 5 (most tortuous; *bottom*).

tures are summarized in three ways in both instances as the maximum, mean, or sum of these changes in chord length and are standardized in two ways by chord length or the square of the chord length. This combination of $2 \times 3 \times 2$ yields 12 indices. The two further indices of tortuosity are based on the angular change in curvature between successive points on the vessel axes and have been detailed previously.²² For ease of image processing, vessels were identified and measured from a circle 120 pixels in diameter, centered on the origin of the optic nerve head (as perceived by the operator [RM]). There was no evidence that any of the tortuosity indices were altered when measured from a circle positioned manually at the rim of the optic nerve head or from a fixed circle 120 pixels in diameter (equivalent to 1.8 mm in the objective plane of an emmetropic eye, chosen to include all sizes of optic nerve head; data not presented). Measures of vessel tortuosity were obtained for all vessels, for arteries and veins, and for the different levels of bifurcation (i.e., primary, secondary, or tertiary branches of the vessel as agreed by subjective assessment). For each image, detection of vessel axes and the measure of tortuosity outlined are obtained within seconds using the computer hardware currently available. It was hypothesized that each of the 14 objective indices would show positive associations with subjective grades. However, there was no a priori hypothesis as to the nature of the association (i.e., whether there was a direct, squared, or logarithmic relationship).

Statistical Analysis

Statistical analyses were performed with commercial software (STATA/SE software, Stata/SE 10 for Windows; StataCorp LP, College Station, TX). Interobserver agreement for subjective assessment of arteriole-venular status, level of branching (1°, 2°, or 3°), and grade of tortuosity was assessed by comparing the proportion of absolute agreements, and agreements within ± 1 for branching and tortuosity grades, as well as κ statistics.²³ Agreement was assessed before grades were combined; the mean grade was used to compare with CAIAR measures. Tortuosity indices from the program demonstrated a positively skewed distribution and hence are summarized by reporting median and interquartile ranges (i.e., from the 25th and 75th percentiles). Tortuosity indices were log transformed before analysis, to normalize distributions. Levels of agreement with subjective grading were quantified by the correlation coefficient and corresponding z -values from the regression (as the probabilities were all very small, $P < 0.001$ in most cases). We repeated the analyses allowing for the inherent correlation within eye and within person using a multilevel model approach, which gave similar results. Hence, simpler regression analyses without multilevel models are presented throughout. Intersession repeatability of tortuosity indices (comparing morning and afternoon sessions of measurement) were assessed in a separate sample by plotting the mean index of tortuosity for the two sessions against the difference between sessions, allowing repeatability over the range of measurement to be gauged.²⁴ Reference ranges (defined as mean difference $\pm 2 \times$ SD) were compared to equivalent differences in subjective grades.

RESULTS

In all, 387 vessel segments of the retina (193 arterioles and 194 venules) from 28 eyes of 14 children (8 white, 3 South Asian, 3 of other ethnic origin; mean age 10 years) were assessed.

Subjective Assessment

The two observers agreed on arteriole-venule status for 191/193 arterioles and 187/194 venules (overall agreement 98%, $\kappa = 0.95$). Disagreements were due to errors in classifying overlapping vessels near the optic nerve head. For primary, secondary, and tertiary branches, observers agreed in 95% (368/387) of classifications ($\kappa = 0.90$); the remaining disagreements differed by only one level of bifurcation. This result was mostly due to errors in classifying vessels that branched at the

beginning of the measurement area. Total agreement was obtained for arteriole-vein and branch status, once grades that differed were convened. For assessment of tortuosity, complete agreement was achieved in 56% of all grades and a further 42% differed by only one grade (κ for agreement within 1 grade 0.97). Only grades that differed by >1 grade (2%) were reassessed by both observers until agreement was reached within ± 1 grade. After reassessment, complete agreement was reached in 57% of grades, and the remainder differed by one grade. Agreement was similar in arterioles (median grade 2, IQR 1-2.5, Table 1) and venules (median grade 1.5, IQR 1-2).

Tortuosity Measures

Table 1 summarizes the 14 tortuosity measures (median and IQR) from the CAIAR program for arterioles and venules combined and gives median values for each index by subjective grade (from 0 to 5). Absolute values varied considerably across the tortuosity indices, with overall median values differing by a factor in excess of 10,000 across the largest chord-based index (in particular, the level-wise—square of the sum of chord length measure) and smallest curvature-based method.²² It is noteworthy that absolute values are somewhat arbitrary, with the large variation across indices being a consequence both of each index quantifying the vessel segment in different ways and also of the different units and different normalizations that arise from the different aggregation schemes used. Hence, absolute values are not used to compare between different indices. All indices returned higher levels of tortuosity for arterioles compared to venules (A/V ratios >1), except segment-wise measures, of which two of the six measures showed higher levels of tortuosity for venules (i.e., ratios <1 ; data not presented). To assess agreement we plotted the log-transformed CAIAR indices individually against the mean subjective grade. A plot of a log-transformed chord length measure of tortuosity (using the mean change in chord length in pixels after repeated bisections of the chord; so-called level-wise mean) against subjective grades is shown in Figure 3. The box-and-whisker plot shows the index (portrayed vertically, showing median and interquartile range) by average subjective grade (from 0 to 5). The log-transformed median values for the index (shown by the black bar in each box) appear to show a linear association with subjective grade. The association at higher subjective grades (grade >3) is less clear due to an insufficient number of observations. Associations observed with other indices, especially segment-wise and curvature-based forms of assessment, appeared to be less good. As a formal examination of the association of log-transformed CAIAR indices with subjective grades, the z -values from linear regression models are given in Table 1. All probabilities for the associations were $P < 0.001$ and hence are not listed, except for the association with segment-wise measures where one of the six indices (based on the square of the maximum difference in chord length) was $P = 0.003$. Level-wise tortuosity measures showed the best agreement with subjective grades ($z > 16$, equivalent to $P = 1.0 \times 10^{-15}$), with curvature-based and segment-wise indices showing weaker agreement. The level-wise-mean index method showed optimal agreement with subjective grades ($z = 24.1$, $r = 0.77$).

Intersession Repeatability

Repeatability of measurements in morning and afternoon sessions approximately 5 hours apart was assessed in 19 children. The mean differences (95% reference range) between sessions of measurement for each tortuosity index are shown in Table 2. The limits of intersession repeatability varied across the 14 indices, but all showed similar levels of agreement across the range of measurement. (Plots of mean versus mean differences

TABLE 1. Summary of the 14 Tortuosity Measures (Median and IQR) from the CAIAR Program for Arterioles and Venules Combined, with Median Values for each Index by Subjective Grade (from 0 to 5)

Objective Measure of Tortuosity	Agreed Subjective Tortuosity Grade										Overall Median (IQR)	Z-value	r	
	0.0 n = 25	0.5 n = 36	1.0 n = 95	1.5 n = 74	2.0 n = 64	2.5 n = 36	3.0 n = 30	3.5 n = 18	4.0 n = 4	4.5 n = 4				5 n = 1
Chord length methods														
Level wise														
Max	0.006	0.007	0.011	0.013	0.023	0.029	0.034	0.057	0.075	0.061	0.121	0.014 (0.009-0.026)	20.40	0.72
Mean	0.003	0.003	0.005	0.006	0.008	0.012	0.013	0.019	0.028	0.018	0.027	0.006 (0.004-0.010)	24.10	0.77
Sum	0.014	0.019	0.030	0.038	0.049	0.071	0.089	0.122	0.157	0.124	0.191	0.039 (0.026-0.063)	23.90	0.77
Maximum ²	0.94	1.19	2.55	3.01	3.73	5.34	7.38	10.88	15.58	12.62	38.33	2.85 (1.71-5.34)	17.00	0.65
Mean ²	0.37	0.50	1.11	1.39	1.41	1.96	2.93	3.52	4.94	3.67	9.08	1.27 (0.79-2.05)	18.70	0.69
Sum ²	2.34	2.98	6.98	9.01	8.49	12.67	20.48	22.09	32.08	22.02	63.57	8.11 (4.65-13.18)	16.54	0.64
Segment wise														
Max	0.031	0.042	0.051	0.052	0.050	0.061	0.079	0.104	0.132	0.125	0.357	0.053 (0.032-0.077)	9.18	0.42
Mean	0.005	0.005	0.006	0.006	0.006	0.007	0.008	0.009	0.014	0.012	0.014	0.006 (0.005-0.008)	11.25	0.5
Sum	0.199	0.259	0.522	0.658	0.409	0.532	0.940	0.820	1.074	0.751	1.722	0.504 (0.268-0.835)	7.71	0.37
Maximum ²	0.005	0.007	0.010	0.010	0.007	0.007	0.014	0.011	0.015	0.011	0.028	0.009 (0.005-0.014)	2.96	0.15
Mean ²	0.001	0.001	0.001	0.001	0.001	0.001	0.001	0.001	0.001	0.001	0.001	0.001 (0.001-0.001)	3.76	0.19
Sum ²	0.039	0.031	0.090	0.104	0.050	0.072	0.112	0.108	0.131	0.132	0.132	0.080 (0.031-0.132)	3.81	0.19
Angular change in curvature														
Hart's 1st method	0.015	0.014	0.016	0.016	0.018	0.025	0.025	0.036	0.035	0.109	0.206	0.018 (0.014-0.026)	10.39	0.44
Hart's 2nd method	0.000	0.000	0.001	0.001	0.001	0.001	0.001	0.007	0.003	0.055	0.130	0.001 (0.000-0.001)	9.58	0.42

n = number of blood vessels measured; IQR, interquartile range; Z-value and r (correlation coefficient) for association with subjective grade.

Units of tortuosity are arbitrary (dependent on the aggregation scheme).

Z-values for linear regression of log-transformed tortuosity index versus subjective grade (where higher z-values show stronger associations), and correlation coefficients (r-value) are also given.

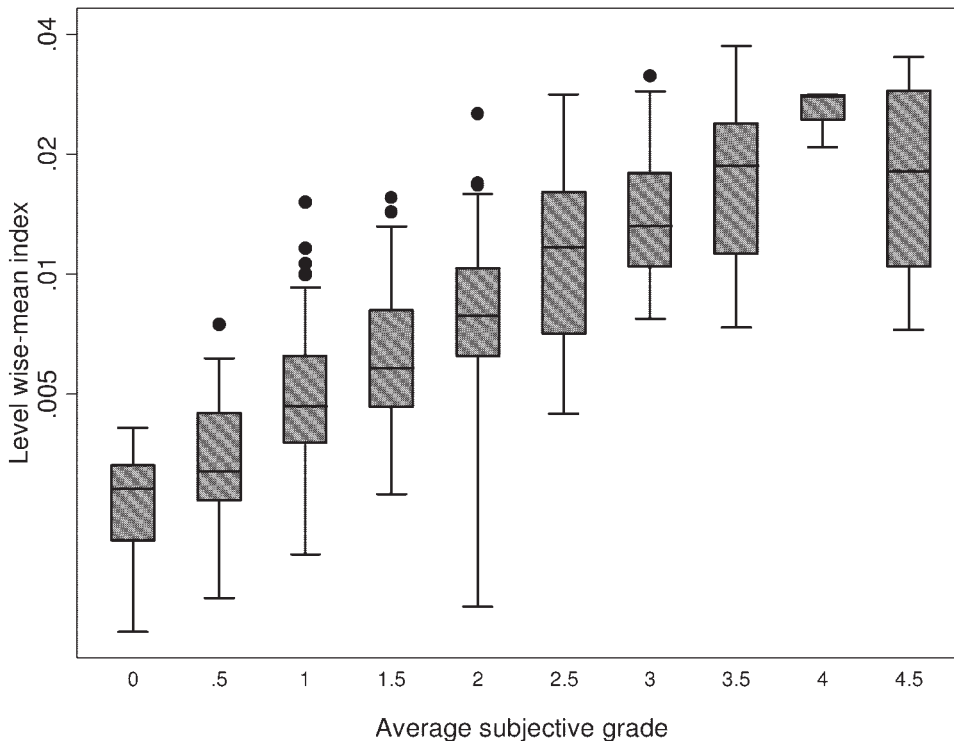


FIGURE 3. Box-and-whisker plot of the level-wise-mean index of tortuosity (portrayed vertically on a log scale; *box* showing median and interquartile range [IQR], *whiskers* showing adjacent values $1.5 \times$ IQR higher than the 75th percentile and $1.5 \times$ IQR lower than the 25th percentile) by agreed subjective grade.

between sessions of measurement are available from the authors.) Comparison of median values for subjective grades 1 and 2 (representing the IQR for all subjective vessel grades) showed that the reference ranges (Table 2) were equivalent to approximately ± 1 subjective grade for the first three level-wise indices (<1 for the level wise-mean index), 2 to 4 grades for three squared level-wise indices. Segment-wise and curvature-based indices performed less well.

DISCUSSION

In this cross-sectional study of 10-year-old children, we examined the agreement between subjective assessment and auto-

TABLE 2. Mean Difference and 95% Reference Range of Intersession Repeatability, for Each Index from the CAIAR Program

Objective Measure of Tortuosity	MD (95% RR)
Chord length methods	
Level wise	
Max	0.000 (-0.013 to 0.013)
Mean	0.000 (-0.003 to 0.003)
Sum	-0.001 (-0.024 to 0.023)
Maximum ²	-0.055 (-3.021 to 2.912)
Mean ²	-0.031 (-0.872 to 0.810)
Sum ²	-0.183 (-6.307 to 5.942)
Segment wise	
Max	-0.001 (-0.082 to 0.079)
Mean	0.000 (-0.004 to 0.004)
Sum	-0.010 (-0.521 to 0.502)
Maximum ²	0.000 (-0.019 to 0.019)
Mean ²	0.000 (-0.001 to 0.001)
Sum ²	0.000 (-0.122 to 0.122)
Angular change in curvature	
Hart's 1st method	-0.001 (-0.123 to 0.121)
Harts 2nd method	0.000 (-0.087 to 0.087)

Mean difference (MD) session 1 - session 2.
 Reference range (RR) = MD \pm 2 \times SD.
 Units of tortuosity are arbitrary (dependent on the aggregation scheme).

rated measures of tortuosity obtained from a dedicated software program (CAIAR). Measures based on subdivided chord lengths showed optimal agreement with subjective assessment (with correlation coefficients in excess of 0.7) and performed better than curvature-based methods.²² These findings in this population-based sample of children with retinal vessels exhibiting a limited range of tortuosity replicate those observed in the assessment of more tortuous retinal vessels of infants with retinopathy of prematurity.¹⁸

Discriminating between tortuous vessels and smoothly curved vessels is a key feature of any clinical assessment of tortuosity.¹⁷ Different methods of quantifying tortuosity exist and may be suited to describing different levels of vessel compromise, ranging from healthy to an overtly diseased state.^{6,15-18} However, the panacea is to use a measure that discriminates between all levels of tortuosity. The CAIAR program returns 14 different measures of tortuosity and was developed to quantify highly tortuous vessels associated with retinopathy of prematurity.¹⁸ We have shown that the program can also be useful in describing retinal vessels in a sample of children from an urban population, who exhibit a more limited range of retinal vessel tortuosity. The method used (based on a level-wise square of the sum of chord length approach) shows a strong correlation with subjective assessment, and demonstrates the well-known clinical observation that retinal arterioles are more tortuous than venules (by as much as a third, when measured subjectively, by 50% when the preferred index is used), and exhibits acceptable levels of intersession repeatability (equivalent to being within ± 1 grade when using the clinical grading scheme outlined). Although a log-linear association was observed, we were uncertain as to the nature of the association when we embarked on this validation study. In the absence of a gold standard, subjective assessment with a detailed protocol was used. Until a gold standard approach is universally adopted, it is likely that subjective assessment will continue to be used. However, in the future it may be useful to compare novel approaches of measuring vessels to those that are shown to optimally agree with subjective clinical assessment. The preferred chord-length-based indices have also

been shown to measure sinusoidal wave forms, simulated to represent vessels ranging from non- to highly tortuous.¹⁸ Dimensional methods of quantifying tortuosity in the CAIAR program that aggregate the changes in chord length over the whole vessel segment (using the mean or sum) may be more reliable than those that measure the maximum change from any of the chord subdivisions, since the latter will be more sensitive to localized errors in identification of vessel axes, whereas such errors will be diluted by mean or sum aggregation. So-called segmentation errors in vessel detection are not uncommon, especially in children, in whom prominent arteriole light reflexes often interfere with the identification of vessel axes. Other studies have emphasized the virtues of curvature-based methods of describing vessel tortuosity.^{4,6,9,22} However, findings in this study, in agreement with findings in infants with more tortuous vessels associated with retinopathy of prematurity,¹⁸ suggest that curvature-based methods perform less well, which implies that these measures may be susceptible to errors in the practical implementation of the algorithm, perhaps due to limitations in sampling of vessel axes positions.

Although subjective assessment of retinal vessel tortuosity was also shown to be a reliable form of assessment in this study (showing good interobserver agreement), it is labor intensive (taking each observer a day to grade nearly 400 vessel segments from 14 individuals), which hinders its use in large population studies. Moreover, clinical grading of tortuosity is ordinal, usually on a scale ranging from none or mild to extreme (from 0 to 5 in this study). Conversely, the semiautomated method outlined is faster (taking approximately 3 hours to analyze the same number of vessel segments) and quantifies vessel tortuosity on a continuous scale. Most of this time is taken with operator control to confirm the correct identification of vessel segments of interest. Once vessel segments are identified, image quantification is fast when the CAIAR program is used. In addition to confirming vessel identification, operator time is also needed to classify vessel segments as arteries or veins and branch status. These vessel characteristics are, as yet, not recognized by the program. Although use of the CAIAR program is not fully automated and requires appreciable operator involvement, there is a learning effect to use of the program that reduces the operator time to less than a ¼ of the time taken for subjective assessment. Although this remains a partial obstacle to use in large population studies, it is hoped that further development of the program will result in more reliable vessel segmentation, which may reduce operator time further.

Another feature of the CAIAR program is that in addition to tortuosity indices, it returns measures of vessel width estimated from the maximum-likelihood model fitting, returning the mean SD of Gaussian profiles fitted along the length of vessel segments of interest. Preliminary analysis suggests that CAIAR assessments of width show a good correlation with subjective assessment ($r = 0.8$), a stronger correlation than previously observed with an older version of the program in infants ($r = 0.4$).¹⁸ However, further assessment of the agreement over a range of measures is needed, especially by vessel type, where arterioles with prominent light reflexes often interfere with vessel segmentation and image processing, and in different ethnic groups, where background levels of retinal pigmentation may alter the interpretation of vessel width artifactually. This assessment is the topic of a future paper.

Because of the difficulties that we have outlined in measuring vessel width, we argue that the assessment of tortuosity may be a more robust indicator of vessel morphology compared with measures of width. Automated assessments have related vessel tortuosity to retinopathy of prematurity and size at birth.^{18,19} However, we are not aware of any studies to date

that have used automated approaches to assess retinal vessel tortuosity in relation to risk factors for diabetes in early life. Two small studies that have used automated approaches to examine the association of retinal vessel tortuosity to diabetes in adulthood showed null effects, but the studies may have been too underpowered to show statistically significant findings (with <30 subjects), and the methods of assessing tortuosity were not stated.^{25,26} We suggest that a sufficiently sized study may show less tortuous retinal vessels associated with diabetes due to vessel engorgement, akin to earlier findings of vessel elongation and dilation associated with diabetic macular edema,²⁷ and decreased vessel tortuosity in relation to ischemic heart disease.⁴ Dilation and decreased tortuosity associated with adult diabetes have also been reported in vessels of the conjunctiva.⁹ Whether similar findings will be observed with risk factors for diabetes at an earlier age remains to be established. However, with previously shown differences in retinal vessel morphology in childhood associated with ethnicity (where African-Caribbeans have a poorer measurement profile compared with whites),²⁰ and cardiovascular risk factors,⁸ which mirror observations in adulthood,²⁸⁻³⁰ the accurate assessment of tortuosity may prove to be a useful indicator of vascular function in early life.³¹ With the emergence of ethnic differences in risk factors for diabetes from the first decade of life, particularly with South Asians having greater risk than white Europeans,^{32,33} the CHASE study (with data collected from >1000 children of South Asian, African-Caribbean, and white European origin) offers an opportunity to investigate this further. The next phase of work will establish the usefulness of the preferred index in being able to detect the differences in vessel tortuosity hypothesized, should these differences exist. If an association between vessel tortuosity and risk factors for diabetes from an early age is observed, the potential use of the program as a screening tool in identifying those at risk of disease can then be realized.

Acknowledgements

The authors thank the members of the CHASE study team, in particular Alicja Kiedzik, Devina Jo-Anne Joysurry, and Melanie Prescott, who made the ocular measures; the participating schools, pupils, and parents; and the Birmingham Optical Group (Birmingham, UK) which provided a Nidek NM-200D handheld fundus camera for the duration of the study.

References

1. Wong TY, Klein R, Couper DJ, et al. Retinal microvascular abnormalities and incident stroke: the Atherosclerosis Risk in Communities Study. *Lancet*. 2001;358(9288):1134-1140.
2. Wong TY, Klein R, Sharrett AR, et al. Retinal arteriolar narrowing and risk of coronary heart disease in men and women: the Atherosclerosis Risk in Communities Study. *JAMA*. 2002;287(9):1153-1159.
3. Wong TY, Klein R, Nieto FJ, et al. Retinal microvascular abnormalities and 10-year cardiovascular mortality: a population-based case-control study. *Ophthalmology*. 2003;110(5):933-940.
4. Witt N, Wong TY, Hughes AD, et al. Abnormalities of retinal microvascular structure and risk of mortality from ischemic heart disease and stroke. *Hypertension*. 2006;47(5):975-981.
5. Ikram MK, Janssen JA, Roos AM, et al. Retinal vessel diameters and risk of impaired fasting glucose or diabetes: the Rotterdam Study. *Diabetes*. 2006;55(2):506-510.
6. Gelman R, Martinez-Perez ME, Vanderveen DK, Moskowitz A, Fulton AB. Diagnosis of plus disease in retinopathy of prematurity using Retinal Image Multiscale Analysis. *Invest Ophthalmol Vis Sci*. 2005;46(12):4734-4738.
7. Cheung N, Saw SM, Islam FM, et al. BMI and retinal vascular caliber in children. *Obesity (Silver Spring)*. 2007; 15(1):209-215.

8. Mitchell P, Cheung N, de Haseth K, et al. Blood pressure and retinal arteriolar narrowing in children. *Hypertension*. 2007;49(5):1156-1162.
9. Owen CG, Newsom RS, Rudnicka AR, Barman SA, Woodward EG, Ellis TJ. Diabetes and the tortuosity of vessels of the bulbar conjunctiva. *Ophthalmology*. 2008;115(6):e27-e32.
10. Parr JC, Spears GF. Mathematic relationships between the width of a retinal artery and the widths of its branches. *Am J Ophthalmol*. 1974;77(4):478-483.
11. Parr JC, Spears GF. General caliber of the retinal arteries expressed as the equivalent width of the central retinal artery. *Am J Ophthalmol*. 1974;77(4):472-477.
12. Knudtson MD, Lee KE, Hubbard LD, Wong TY, Klein R, Klein BE. Revised formulas for summarizing retinal vessel diameters. *Curr Eye Res*. 2003;27(3):143-149.
13. Lotmar W, Freiburghaus A, Bracher D. Measurement of vessel tortuosity on fundus photographs. *Albrecht Von Graefes Arch Klin Exp Ophthalmol*. 1979;211(1):49-57.
14. Capowski JJ, Kylstra JA, Freedman SF. A numeric index based on spatial frequency for the tortuosity of retinal vessels and its application to plus disease in retinopathy of prematurity. *Retina*. 1995;15(6):490-500.
15. Koreen S, Gelman R, Martinez-Perez ME, et al. Evaluation of a computer-based system for plus disease diagnosis in retinopathy of prematurity. *Ophthalmology*. 2007;114(12):e59-e67.
16. Wallace DK. Computer-assisted quantification of vascular tortuosity in retinopathy of prematurity (an American Ophthalmological Society thesis). *Trans Am Ophthalmol Soc*. 2007;105:594-615.
17. Grisan E, Foracchia M, Ruggeri A. A novel method for the automatic grading of retinal vessel tortuosity. *IEEE Trans Med Imaging*. 2008;27(3):310-319.
18. Wilson CM, Cocker KD, Moseley MJ, et al. Computerized analysis of retinal vessel width and tortuosity in premature infants. *Invest Ophthalmol Vis Sci*. 2008;49(8):3577-3785.
19. Tapp RJ, Williams C, Witt N, et al. Impact of size at birth on the microvasculature: the Avon Longitudinal Study of Parents and Children. *Pediatrics*. 2007;120(5):e1225-e1228.
20. Tillin T, Evans RM, Witt NW, et al. Ethnic differences in retinal microvascular structure. *Diabetologia*. 2008;51(9):1719-1722.
21. Whincup PH, Owen CG, Orfei L, McKay C, Cook DG. Ethnic differences in risk factors for chronic disease have their origins in early life: evidence for the CHASE study. *Early Hum Dev*. 2007;83(1):S63.
22. Hart WE, Goldbaum M, Cote B, Kube P, Nelson MR. Measurement and classification of retinal vascular tortuosity. *Int J Med Inform*. 1999;53(2-3):239-252.
23. Landis JR, Koch GG. The measurement of observer agreement for categorical data. *Biometrics*. 1977;33(1):159-174.
24. Bland JM, Altman DG. Statistical methods for assessing agreement between two methods of clinical measurement. *Lancet*. 1986;1(8476):307-310.
25. Zhou P, Wang M, Cao H. Research on features of retinal images associated with hypertension and diabetes. *Conf Proc IEEE Eng Med Biol Soc*. 2005;6:6415-6417.
26. Wang X, Cao H, Zhang J. Analysis of retinal images associated with hypertension and diabetes. *Conf Proc IEEE Eng Med Biol Soc*. 2005;6:6407-6410.
27. Kristinsson JK, Gottfredsdottir MS, Stefansson E. Retinal vessel dilatation and elongation precedes diabetic macular oedema. *Br J Ophthalmol*. 1997;81(4):274-278.
28. Leung H, Wang JJ, Rochtchina E, et al. Relationships between age, blood pressure, and retinal vessel diameters in an older population. *Invest Ophthalmol Vis Sci*. 2003;44(7):2900-2904.
29. Wong TY, Islam FM, Klein R, et al. Retinal vascular caliber, cardiovascular risk factors, and inflammation: the Multi-Ethnic Study of Atherosclerosis (MESA). *Invest Ophthalmol Vis Sci*. 2006;47(6):2341-2350.
30. Wong TY, Klein R, Islam FM, et al. Diabetic retinopathy in a multi-ethnic cohort in the United States. *Am J Ophthalmol*. 2006;141(3):446-455.
31. Griffith TM, Edwards DH, Davies RL, Harrison TJ, Evans KT. EDRF coordinates the behaviour of vascular resistance vessels. *Nature*. 1987;329(6138):442-445.
32. Whincup PH, Gilg JA, Papacosta O, et al. Early evidence of ethnic differences in cardiovascular risk: cross sectional comparison of British South Asian and white children. *BMJ*. 2002;324(7338):635.
33. Whincup PH, Gilg JA, Owen CG, Odoki K, Alberti KG, Cook DG. British South Asians aged 13-16 years have higher fasting glucose and insulin levels than Europeans. *Diabet Med*. 2005;22(9):1275-1277.